Polymer Chemistry

Accepted Manuscript

ROYAL SOCIETY OF CHEMISTRY

www.rsc.org/polymers

Cite this: DOI: 10.1039/c0xx00000x

www.rsc.org/xxxxxx

ARTICLE TYPE

Semi-Crystalline Diblock Copolymer Nano-Objects Prepared via RAFT Alcoholic Dispersion Polymerization of Stearyl Methacrylate

Mona Semsarilar, Nicholas J. W. Penfold, Elizabeth R. Jones and Steven P. Armes*

Received (in XXX, XXX) Xth XXXXXXXXX 20XX, Accepted Xth XXXXXXXXX 20XX

DOI: 10.1039/b000000x

Abstract. The RAFT dispersion polymerization of stearyl methacrylate (SMA) is conducted in ethanol at 70°C using a poly(2-(dimethylamino)ethyl methacrylate) [PDMA] chain transfer agent. The growing PSMA block becomes insoluble in ethanol, which leads to polymerization-induced self-assembly (PISA) and hence produces a range of copolymer morphologies depending on the precise $PDMA_y$-$PSMA_x$ formulation. More specifically, pure phases corresponding to either spherical nanoparticles, worm-like nanoparticles or vesicles can be prepared as judged by transmission electron microscopy. However, the worm phase space is relatively narrow, so construction of a detailed phase diagram is required for reproducible syntheses of this morphology. Inter-digitation of the stearyl (C_{18}) side-groups leads to a semi-crystalline PSMA core block and the effect of systematically varying the mean degree of polymerization of both the PDMA and PSMA blocks on the T_m and T_c is investigated using differential scanning calorimetry. Finally, it is demonstrated that these cationic nanoparticles can be employed as colloidal templates for the *in situ* deposition of silica from aqueous solution.

Introduction

Well-defined amphiphilic diblock copolymers and their self-assembly in dilute aqueous solution has been the subject of substantial research over the last two decades.[1-3] The development of living radical polymerization techniques such as reversible addition–fragmentation chain transfer (RAFT) polymerization[4,5] has enabled a wide range of novel block copolymers to be prepared directly using various functional monomers without recourse to protecting group chemistry.[6-10] Traditionally, amphiphilic diblock copolymers have been synthesized and then isolated, with a subsequent separate processing step such as a solvent switch, pH switch, or thin film rehydration being used to induce self-assembly.[2-3,11-13] However, such self-assembly is usually only conducted at relatively low copolymer concentration, which makes the production of diblock copolymer nano-objects somewhat problematic on an industrial scale. Recently, polymerization-induced self-assembly (PISA) has been developed by various research groups.[14-20] This highly attractive approach enables bespoke organic nanoparticles to be prepared directly during the copolymer synthesis at much higher concentrations. The most versatile PISA formulation is based on dispersion polymerization, which can be performed in either water,[21] polar solvents such as alcohols,[22-31] or non-polar solvents such as *n*-alkanes.[32-33] In each case, a soluble macromolecular chain transfer agent (macro-CTA) is chain-extended using a soluble vinyl monomer in a suitable solvent that is a non-solvent for the growing second block. At some critical degree of polymerization, *in situ* nucleation occurs and the growing micelles become swollen with unreacted monomer.[18,20] This high local monomer concentration leads to a significant increase in the rate of polymerization, which ensures that very high monomer conversions are achieved within a few hours.[18,20] Depending on the precise formulation, the final copolymer morphology can be either near-monodisperse spheres, polydisperse worms, or polydisperse vesicles. Worms are produced via the multiple 1D fusion of monomer-swollen spheres, whereas vesicles are formed via the evolution of various copolymer morphologies that include 'jellyfish' intermediates.[18]

Typically, diblock copolymer nano-objects comprise amorphous core-forming polymers such as polystyrene, poly(methyl methacrylate) or poly(2-hydroxypropyl methacrylate).[14,21,27,35] However, semi-crystalline blocks have also been utilized to prepare nanoparticles with liquid crystalline cores.[36-39] To date, we are only aware of one example of a semi-crystalline block being used in a PISA formulation.[40] Potential advantages of using such core-forming blocks could be (i) production of relatively stiff worms whose rigidity could be tuned by varying the temperature and (ii) preparation of vesicles with more impermeable membranes that enable better encapsulation performance.

In the present study, a poly(2-(dimethylamino)ethyl methacrylate) [PDMA] macro-CTA is chain-extended with stearyl methacrylate [SMA] via RAFT alcoholic dispersion polymerization in ethanol at 70 °C (see Scheme 1 overleaf). Unlike the amorphous polystyrene or poly(benzyl methacrylate) [PBzMA] core-forming block previously reported, [14-15, 22-31] the PSMA block is semi-crystalline. Its selection for PISA syntheses was inspired in part by recent studies by Manners and co-workers,[36-39] who have reported a wide range of exotic copolymer morphologies based on the concept of 'living crystallization'. The resulting diblock copolymer nanoparticles are characterized using transmission electron microscopy (TEM), dynamic light scattering (DLS) and differential scanning calorimetry (DSC). Furthermore, a detailed phase diagram is constructed and compared to similar phase diagrams reported for diblock copolymer nano-objects comprising amorphous core-forming blocks. Selected cationic vesicles are also evaluated as colloidal templates for the in situ deposition of silica.

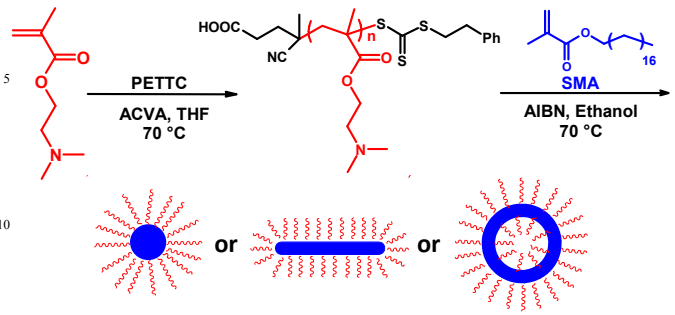

Scheme 1. Synthesis of diblock copolymer nano-objects prepared by RAFT alcoholic dispersion polymerization of stearyl methacrylate (SMA) at 70 °C using a poly(2-(dimethylamino)ethyl methacrylate) chain transfer agent. The final diblock copolymer morphology can be either spheres, worms or vesicles, depending on the precise diblock copolymer composition.

Experimental

Materials

2-(Dimethylamino)ethyl methacrylate (DMA), stearyl methacrylate (SMA) and 4,4′-azobis (4-cyanovaleric acid) (ACVA) were used as received from Sigma Aldrich (UK). Tetrahydrofuran (THF), dichloromethane (DCM) and absolute ethanol were purchased from Fisher Scientific (UK). 2,2′-Azobisisobutyronitrile (AIBN) was recrystallized from methanol. Deuterated dichloromethane (CD_2Cl_2) was purchased from Cambridge Isotope Lab Inc. while 4-cyano-4 (2-phenylethane sulfanylthiocarbonyl)sulfanylpentanoic acid (PETTC) was synthesized in-house according to a literature protocol.[20]

Copolymer characterization

^{1}H NMR Spectroscopy. All NMR spectra were recorded at 300 K using a 400 MHz Bruker Avance-400 spectrometer in $CDCl_3$ (for diblock copolymers) or CD_2Cl_2 (for the PDMA macro-CTA). Sixty-four scans were averaged per spectrum.

Dynamic Light Scattering. All DLS measurements were recorded at 20 °C using a Malvern Instruments Zetasizer Nano series instrument equipped with a 4 mW, 633 nm He−Ne laser and an avalanche photodiode detector. Copolymer dispersions were diluted in ethanol to 1.0% w/w concentration and the scattered light was detected at 173°. A refractive index of 1.49 was used for these measurements.

Gel Permeation Chromatography. 1.0% w/w copolymer solutions were prepared in THF with toluene as the flow rate marker. GPC measurements were conducted using a THF eluent containing 2.0% v/v triethylamine, 0.05% w/v butylhydroxytoluene (BHT) at a flow rate of 1.0 mL min-1 using a WellChrom K-2301 RI detector operating at 950 ± 30 nm. A series of near-monodisperse poly(methyl methacrylate) standards were used for calibration.

Transmission Electron Microscopy. All TEM images were recorded using a 100 kV Phillips CM100 instrument equipped with a Gatan 1K CCD camera. Copper/palladium TEM grids were coated with an ultrathin surface layer of amorphous carbon, then plasma glow-discharged to create a hydrophilic surface. Each alcoholic diblock copolymer sample (0.20% w/w, 10 µL) was negatively stained with a 0.75% w/w aqueous solution of uranyl formate before imaging in order to improve the contrast.

Differential Scanning Calorimetry: Samples were analyzed using a Pyris 1 Perkin-Elmer DSC instrument. Each sample was dried for 48 h in a vacuum oven before a 10 mg sample was analyzed by cycling between 10 °C and 50°C for four cycles. The heating and cooling rates were fixed at 10 °C min^{-1}.

Synthesis of PDMA macro-CTA via solution polymerization in THF.

A round-bottom flask was charged with DMA (10.0 g, 64 mmol), PETTC (0.432 g, 1.27 mmol) and ACVA (0.071 g, 0.254 mmol) before addition of fresh THF (10.0 g). The sealed reaction vessel was purged under nitrogen for 20 min then heated with magnetic stirring using a 70 °C for 7.5 h before quenching by cooling the reaction solution to room temperature and exposing it to air. The resulting polymer solution was purified by extraction (using two 500 ml portions of 40:60 petroleum ether) until the extractions were no longer cloudy. ^{1}H NMR analysis confirmed the absence of residual monomer. The polymer was further dissolved in the minimum amount of DCM, then removed under vacuum until a yellow solid was formed, which was dried in a vacuum oven for 24 h. A mean degree of polymerization (DP) of 55 was confirmed by end group analysis: the aromatic PETTC signals at 7.4 ppm were compared to those assigned to the polymer backbone at 4.0-4.5 ppm using ^{1}H NMR spectroscopy. The same protocol was used to prepare a $PDMA_{65}$ macro-CTA using DMA (20.0 g, 127 mmol), PETTC (0.539 g, 1.59 mmol), ACVA (44.0 mg, 0.159 mmol) and THF (20 g). An ACVA/PETTC molar ratio of 10 was utilized in each macro-CTA synthesis.

Synthesis of $PDMA_{65}$-$PSMA_x$ at diblock copolymer particles via RAFT dispersion polymerization in ethanol at 70 °C.

In a typical protocol for the synthesis of $PDMA_{65}$-$PSMA_{75}$ at 15% w/w solids: $PDMA_{65}$ (0.17 g, 0.017 mmol), SMA (0.40 g, 1.18 mmol) and AIBN (0.45 mg, 0.032 mmol) were dissolved in ethanol (3.13 g, 67.8 mmol) to produce a transparent yellow solution, which was purged under N_2 for 20 min. The sealed solution was heated in a preheated oil bath at 70 °C for 24 h, then exposed to air and cooled to room temperature to quench the SMA polymerization. ^{1}H NMR analysis was used to determine the final monomer conversion. A series of diblock copolymers was synthesized over a range of PSMA DPs at various solids concentrations by systematic variation of the SMA/PDMA molar ratio and ethanol content, respectively.

Fabrication of hybrid silica-coated copolymer nanoparticles at 60 °C.

A continuously stirred ethanolic dispersion of copolymer particles was diluted from 30.0 to 0.25% w/w by the addition of water. 1.0 mL of this dispersion was adjusted to pH 2 (by addition of HCl), mixed with 1.0 mL of a 1.0 g dm^{-3} aqueous lysine solution and heated to 60 °C. TEOS was then added and the reaction mixture was continuously stirred for 18 h at this temperature. The hybrid silica/polymer particles were purified via

three centrifugation-redispersion cycles in water, with redispersion being aided by ultrasonication.

Results and Discussion

Over the last five years or so, PISA has become widely recognized as a highly versatile technique for the efficient synthesis of sterically-stabilized diblock copolymer nanoparticles of various morphologies in relatively concentrated solution.[14-35] For alcoholic dispersion polymerization formulations, we have examined using PBzMA as the core-forming block.[22-26] For example, a detailed phase diagram has been reported for PDMA-PBzMA diblock copolymers prepared via RAFT dispersion polymerization of BzMA in ethanol.[23] In the present study, this prototypical amorphous core-forming block has been replaced with semi-crystalline poly(stearyl methacrylate) (PSMA). Fundamental questions which we wished to address were whether this switch still enabled PISA syntheses to be conducted and, if so, to what extent was the phase diagram affected. As shown in Scheme 1, a PDMA macro-CTA with a mean DP of 55 (M_n = 8,700 g mol^{-1}, M_w = 10,500 g mol^{-1}, M_w/M_n = 1.20) was prepared via RAFT solution polymerization in THF and then chain-extended with SMA in ethanol at 70°C to produce a series of $PDMA_{55}$-$PSMA_x$ diblock copolymers via RAFT dispersion polymerization. Since the PSMA chains are insoluble in ethanol, a range of copolymer morphologies can be generated via *in situ* self-assembly simply by varying the DP of the PSMA chain, since this affects the relative block volume fractions and hence the overall packing parameter.[41] In each case the alcohol-soluble PDMA chains act as an effective steric stabilizer for the diblock copolymer nanoparticles.

A kinetic study of the SMA polymerization was conducted when targeting a DP of 100 for the core-forming block (Figure 1). ^{1}H NMR analysis indicated that a SMA conversion of 82% was obtained after 14 h, with essentially full conversion being achieved after 24 h. The evolution of molecular weight with conversion was also monitored to assess the living character of the SMA polymerization (see Figure 2). The observed linear relationship indicates a well-controlled pseudo-living RAFT polymerization. Polydispersities remained between 1.20 and 1.26 throughout the reaction, with the targeted $PDMA_{55}$–$PBzMA_{100}$ diblock copolymer having a final M_w/M_n of 1.25. GPC traces were invariably unimodal with little or no tailing, which indicated a relatively high blocking efficiency and suggested that relatively few copolymer chains were terminated prematurely (see Figure 3).

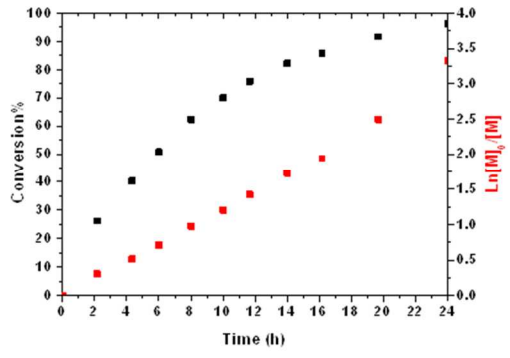

Figure 1. Kinetic data obtained for the RAFT dispersion polymerization of SMA at 20% w/w solids in ethanol at 70 °C using a $PDMA_{55}$ macro-CTA at a macro-CTA/AIBN molar ratio of 5.0. The targeted diblock composition was $PDMA_{55}$–$PSMA_{100}$.

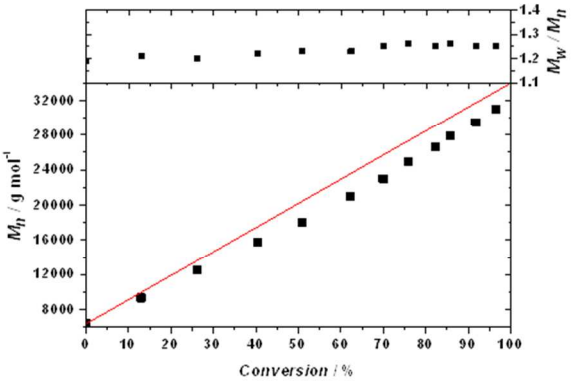

Figure 2. Evolution of number-average molecular weight (M_n) and polydispersity (M_w/M_n) with conversion for the RAFT dispersion polymerization of SMA at 20% w/w solids in ethanol at 70 °C using a $PDMA_{55}$ macro-CTA and a macro-CTA/AIBN molar ratio of 5.0, as judged by THF GPC (vs. poly(methyl methacrylate) calibration standards). The targeted diblock composition was $PDMA_{55}$–$PSMA_{100}$.

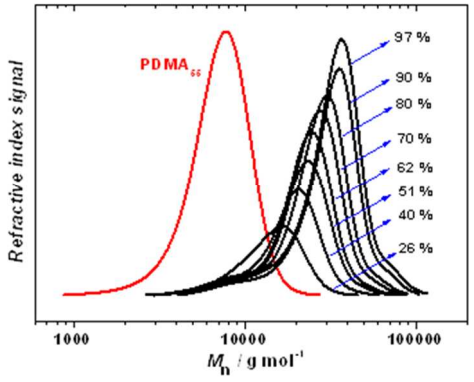

Figure 3. GPC curves recorded using a refractive index detector during the RAFT dispersion polymerization of SMA at 20% w/w solids in ethanol at 70 °C using a $PDMA_{55}$ macro-CTA and a macro-CTA/AIBN molar ratio of 5.0. The targeted diblock composition was $PDMA_{55}$-$PSMA_{100}$.

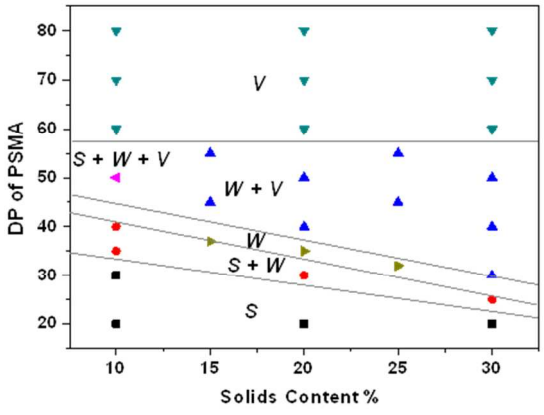

Figure 4. Phase diagram constructed for $PDMA_{55}$-$PSMA_x$ RAFT alcoholic dispersion polymerization formulation by systematic variation of the mean target DP of $PSMA_x$ and the total solids concentration (expressed as % w/w) [S = spheres, W = worms and V = vesicles].

A large batch of $PDMA_{55}$ macro-CTA was synthesized to ensure that the stabilizer block DP was held constant while systematically varying the core-forming block DP for the preparation of the diblock copolymer nanoparticles. The second variable used to construct the phase diagram shown in Figure 4 was the total copolymer concentration used for the SMA polymerization: this parameter was varied from 10 to 30% w/w solids. For a given DP of the macro-CTA, the core-forming block DP dictates the packing parameter of the diblock copolymer chains, which in turn determines the final copolymer morphology (as judged by *post mortem* TEM studies). For most of the copolymer concentrations investigated, a gradual evolution from spheres to worms to vesicles is observed as the target DP of the PSMA chains is increased, with mixed phases always being observed between the three pure phases. This is illustrated in Figure 5, which depicts a series of TEM images (5a to 5d) recorded for SMA polymerizations conducted at 20 % w/w solids. A mixed phase of spheres and short worms are obtained at a mean PSMA DP of 30, while an unusually narrow pure worm phase is identified for a DP of 35. This observation is attributed to the relatively high molar mass (310.5 g mol^{-1}) of the SMA repeat units. A worm plus vesicle mixed phase is observed at a mean PSMA DP of 50, while a pure vesicle phase is produced when targeting a $PDMA_{55}$–$PSMA_{70}$ diblock composition. The same general behavior is observed at each of the concentrations investigated in this study, see Figure 4. The RAFT alcoholic dispersion formulation enables vesicles to be generated at just 10% solids, which suggests that the copolymer concentration has a relatively weak influence on particle morphology. Similar findings were reported by Jones et al. for a $PDMA_{31}$-$PBzMA_x$ formulation.[23] Figures 5e to 5h illustrate the gradual change in copolymer morphology that occurs when targeting a PSMA DP of 30-33 at various copolymer concentrations (10-30 % w/w solids). In contrast, at a higher PSMA DP of 60 a pure vesicle phase was obtained, regardless of the copolymer concentration. All ancillary experimental results (e.g. DLS particle diameters and THF GPC data) associated with the phase diagram shown in Figure 4 are summarized in Table S1 (see Supporting Information). The spherical diblock copolymer nanoparticles can exhibit relatively narrow size distributions (e.g. see Figure 5e), whereas worms or vesicles (or mixed phases) invariably possess significantly higher polydispersities.

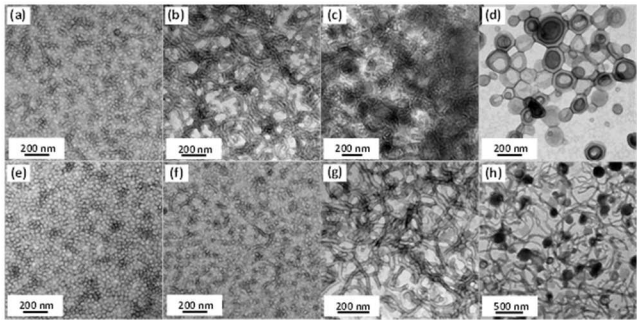

Figure 5. TEM images obtained for: (a) $PDMA_{55}$-$PSMA_{30}$ at 20%; (b) $PDMA_{55}$-$PSMA_{35}$ at 20%; (c) $PDMA_{55}$-$PSMA_{50}$ at 20%; (d) $PDMA_{55}$-$PSMA_{70}$ at 20%; (e) $PDMA_{55}$-$PSMA_{30}$ at 10%; (f) $PDMA_{55}$-$PSMA_{30}$ at 19%; (g) $PDMA_{55}$-$PSMA_{33}$ at 25%; (h) $PDMA_{55}$-$PSMA_{30}$ at 30%.

It is perhaps worth emphasizing that the Stokes-Einstein equation is only strictly valid for spherical particles, hence the DLS technique reports a 'sphere-equivalent' diameter and should be treated with caution when used to characterize the worm phase. The relatively high vesicle polydispersities indicated by DLS studies are consistent with the corresponding TEM images obtained for these samples; similar results have been reported by other workers.[14-15, 27-28] Regardless of the final copolymer morphology, GPC analysis of the diblock copolymer chains yielded monomodal curves with little or no tailing, suggesting high blocking efficiencies and relatively well-controlled RAFT polymerizations.

We also examined the possibility of extending the pure worm phase by employing a somewhat longer stabilizer block. Thus a PDMA macro-CTA with a mean DP of 65 was prepared on a multi-gram scale and used to construct a second phase diagram. Inspecting Figure S1, it is clear that increasing the mean stabilizer DP by just 10 units produces a significantly broader pure worm phase (which exists at a DP of between 60 and 70 at 20-25 % solids). Again, all ancillary experimental results (including DLS particle diameters and THF GPC data) associated with this second phase diagram are summarized in Table S2 (see Supporting Information).

Table 1. Characteristic thermal transitions T_m and T_c determined for the crystalline and amorphous transitions respectively for (i) $PDMA_y$-$PSMA_x$ diblock copolymer nano-objects prepared at 20% w/w solids via RAFT alcoholic dispersion polymerization at 70 °C and (ii) the corresponding $PSMA_{30\text{-}60}$ homopolymers prepared by RAFT solution polymerization at 70 °C in toluene.

Copolymer composition	TEM morphology	T_m (°C)	T_c (°C)
$PSMA_{30}$	-	31.0	17.7
$PSMA_{40}$	-	31.4	17.8
$PSMA_{60}$	-	32.1	18.9
$PDMA_{55}$-$PSMA_{30}$	spheres	28.1	15.4
$PDMA_{55}$-$PSMA_{40}$	worms	29.1	15.1
$PDMA_{55}$-$PSMA_{60}$	vesicles	29.5	17.1
$PDMA_{65}$-$PSMA_{50}$	spheres	27.2	16.0
$PDMA_{65}$-$PSMA_{65}$	worms	27.6	15.5
$PDMA_{65}$-$PSMA_{70}$	worms	28.1	15.7
$PDMA_{65}$-$PSMA_{110}$	vesicles	28.7	17.1

DSC was used to identify the critical temperature at which the semi-crystalline PSMA block becomes amorphous. In principle, the diblock copolymer morphology could affect this thermal transition. Thus the samples selected for DSC analysis included all three copolymer morphologies (i.e. spheres, worms and vesicles), as well as three PSMA homopolymers. All samples were subjected to four heating cycles between 10 °C and 50 °C at a heating rate of 10 °C min^{-1}. The first heating cycle was performed to remove any hysteresis effects. T_m and T_c are the characteristic temperatures at which the crystalline PSMA phase becomes amorphous and the amorphous PSMA phase becomes crystalline, respectively.[42,43] Figure S2 shows the normalized heat flow vs. temperature and the endothermic T_m peaks. The three PSMA homopolymers with mean DPs of 30, 40 or 60 exhibit T_m

values ranging from 31.0 °C to 32.1 °C, indicating a relatively weak molecular weight dependence. A modest increase in T_m from 28.1 °C to 29.5 °C (for the $PDMA_{55}$-$PSMA_x$ copolymer series) and 27.2 °C to 28.7 °C (for the $PDMA_{65}$-$PSMA_x$ copolymer series) was observed on increasing the DP of the PSMA block from 30 to 60 or from 50 to 110, respectively (see Table 1). These relatively small differences in T_m (~ 1.4-1.5 °C) seem to be mainly the result of the increasing DP of the PSMA block, although subtle effects owing to differing copolymer morphologies (i.e. spheres, worms or vesicles) cannot be ruled out. The T_c data determined for various diblock copolymers (see Table 1) show a similar trend, whereby values for the $PDMA_{55}$-$PSMA_x$ diblock copolymers are slightly lower (~2-3 °C) than those for the corresponding $PSMA_x$ homopolymer (where x = 30, 40 or 60). During these PISA syntheses, it was noticed that the diblock copolymer morphologies were somewhat less turbid during polymerization of SMA at 70 °C than after cooling to room temperature. To examine whether this phenomenon is related to a change in the degree of solvation of the core-forming block, two different copolymer compositions representing spheres and vesicles were analyzed by variable temperature ^{1}H NMR spectroscopy, as shown in Figure 6. All spectra were recorded in C_2D_5OD, thus only the PDMA stabilizer signals were expected to be visible since the core-forming PSMA chains are insoluble in this solvent. Close inspection of the two series of spectra obtained for the spherical and vesicular particles indicates that, on heating from 25 °C to 60 °C, the signal at 1.35 ppm become more prominent. This suggests that the spherical particle cores and vesicle membranes each become partially solvated, which is consistent with the observed reduction in turbidity of these dispersions.

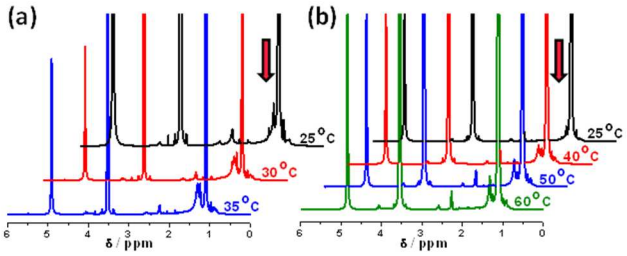

Figure 6. ^{1}H NMR spectra recorded for (a) $PDMA_{55}$-$PSMA_{76}$ vesicles prepared at 10% w/w solids in $(CD_3)_2CDOD$ and (b) $PDMA_{55}$-$PSMA_{40}$ spheres prepared at 10% w/w solids in C_2D_5OD.

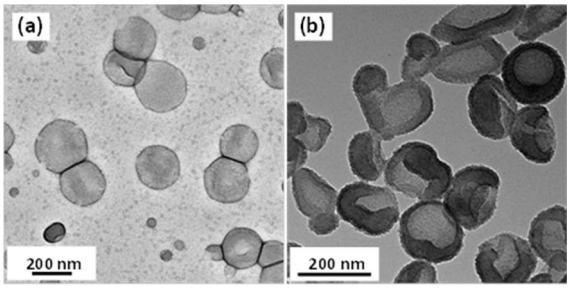

Figure 7. TEM images obtained for: (a) $PDMA_{55}$-$PSMA_{93}$ diblock copolymer vesicles prepared at 20% w/w solids in ethanol, (b) the same vesicles after silicification using 1.5 eq. TEOS. The silicified vesicles were not stained prior to TEM imaging since the relatively dense silica shell provides sufficient electron contrast.

We have previously reported that diblock copolymer nano-objects prepared using a PDMA macro-CTA in ethanol acquire cationic surface charge on transfer into acidic aqueous media (e.g. by dialysis) as a result of protonation of the PDMA stabilizer chains. In principle, this cationic surface charge should be capable of catalysing the hydrolysis and polycondensation of a soluble silica precursor (TEOS) to form silica-coated nanoparticles.[44] Accordingly, TEOS was added to an acidic dispersion (pH 2) containing 0.25 wt. % $PDMA_{55}$-$PSMA_{93}$ vesicles (see Figure 7a). Lysine (1.4 mg/mL) was also added to facilitate silica deposition.[45]

TEM images of the resulting hybrid $PDMA_{55}$-$PSMA_{93}$ vesicles are shown in Figure 7b, where a uniform layer of silica is clearly visible on the particle surface. Unlike the precursor vesicles, these silica-clad vesicles required no TEM staining since the relatively high density of the inorganic over layer confers sufficient electron contrast. DLS studies of the $PDMA_{55}$-$PSMA_{93}$ diblock copolymer precursor vesicles gave an intensity-average diameter of 180 nm and a polydispersity of 0.06, indicating a relatively narrow particle size distribution. DLS analysis of the corresponding silica-clad $PDMA_{55}$-$PSMA_{93}$ vesicles indicated an intensity-average diameter of 195 nm and a similarly low polydispersity (0.05). Thus the silica-clad vesicles can retain their colloidal stability in aqueous solution provided that the deposited silica overlayer is not too thick.

Conclusions

In summary, two poly(2-(dimethylamino)ethyl methacrylate) (PDMA) macro-CTAs were chain-extended via RAFT dispersion polymerization of stearyl methacrylate (SMA) at 70 °C in ethanol. Kinetic experiments confirmed that high conversions were achieved within 24 h, while GPC analyses indicated well-controlled polymerizations and TEM studies revealed well-defined diblock copolymer nanoparticles. Macro-CTAs with mean DPs of either 55 or 65 were used to construct detailed phase diagrams, which are essential for the reproducible synthesis of pure copolymer morphologies. Using the longer PDMA macro-CTA gave a broader pure worm phase compared to the shorter macro-CTA. Comparing these two phase diagrams, it is apparent that the final copolymer morphology is very sensitive to the DP of the core-forming PSMA block, but rather less sensitive to the overall copolymer concentration. Differential scanning calorimetry studies on the diblock copolymer particles indicated that both T_m and T_c are slightly lower than the characteristic thermal transitions obtained for the corresponding PSMA homopolymers. However, T_m was sensitive to the PSMA DP, whereas T_c appears to depend the on the diblock copolymer morphology. $PDMA_{55}$-$PSMA_{93}$ vesicles were successfully utilized as a colloidal template for the deposition of silica via hydrolysis of a TEOS precursor in the presence of lysine.

Acknowledgments

EPSRC is thanked for post-doctoral support of MS (EP/G007950/1). SPA acknowledges a five-year ERC Advanced Investigator grant (PISA: 320372).

Notes and references

Department of Chemistry, University of Sheffield, Brook Hill, Sheffield, South Yorkshire, S3 7HF, UK. *s.p.armes@sheffield.ac.uk

†Electronic Supplementary Information (ESI) available: Monomer conversions, intensity-average particle diameters, molecular weight data, copolymer morphologies and DSC traces. See DOI: 10.1039/b000000x/

1 Y. Mai and A. Eisenberg, *Chem. Soc. Rev*., 2012, **41**, 5969.
2 L. Zhang and A. Eisenberg, *Science*, 1995, **268**, 1728.
3 L. Zhang and A. Eisenberg, *J. Am. Chem. Soc*., 1996, **118**, 3168.
4 J. Chiefari, Y. K. Chong, F. Ercole, J. Krstina, J. Jeffery, T. P. T. Le, R. T. A. Mayadunne, G. F. Meijs, C. L. Moad, G. Moad, E. Rizzardo and S. H. Thang, *Macromolecules*, 1998, **31**, 5559.
5 G. Moad, E. Rizzardo and S. H. Thang, *Polymer*, 2008, **49**, 1079.
6 N. Tirelli, M. P. Lutolf, A. Napoli and J. A. Hubbell, *Rev. Mol. Biotechnol.*, 2002, **90**, 3.
7 A. E. Smith, X. Xu and C. L. McCormick, *Prog. Polym. Sci*., 2010, **35**, 45.
8 C. Barner-Kowollik, J. P. Blinco and S. Perrier, *Synthesis of Polymers*, 2012, **2**, 601.
9 A. B. Lowe and C. L. McCormick, *Prog. Polym. Sci*., 2007, **32**, 283.
10 C. Boyer, M. H. Stenzel and T. P. Davis, *J. Polym. Sci. Part A: Polym. Chem.*, 2011, **49**, 551.
11 R. C. Hayward and D. J. Pochan, *Macromolecules*, 2010, **43**, 3577.
12 X. Wang, G. Guerin, H. Wang, Y. Wang, I. Manners and M. A. Winnik, *Science*, 2007, **317**, 644.
13 H. Cui, Z. Chen, S. Zhong, K. L. Wooley and D. J. Pochan, *Science*, 2007, **317**, 647.
14 S. Boisse, J. Rieger, K. Belal, A. Di-Cicco, P. Beaunier, M.- H. Li and B.Charleux, *Chem. Commun.*, 2010, **46**, 1950.
15 X. Zhang, S. Boisse, W. Zhang, P. Beaunier, F. D'Agosto, J. Rieger and B. Charleux, *Macromolecules*, 2011, **44**, 4149.
16 Y. Li and S. P. Armes, *Angew. Chem. Int. Ed*., 2010, **49**, 4042.
17 S. Sugihara, A. Blanazs, S. P. Armes, A. J. Ryan and A. L. Lewis, *J. Am. Chem. Soc.*, 2011, **133**, 15707.
18 A. Blanazs, J. Madsen, G. Battaglia, A. J. Ryan and S. P. Armes, *J. Am. Chem. Soc.*, 2011, **133**, 16581.
19 V. Ladmiral, M. Semsarilar, I. Canton and S. P. Armes, *J. Am. Chem. Soc.*, 2013, **135**, 13574.
20 M. Semsarilar, V. Ladmiral, A.Blanazs and S. P. Armes, *Langmuir*, 2013, **29**, 7416; M. Semsarilar, V. Ladmiral, A. Blanazs and S. P. Armes, *Langmuir*, 2012, **28**, 914.
21 N. J. Warren and S. P. Armes, *J. Am. Chem. Soc*., 2014, **136**, 10174.
22 M. Semsarilar, E. R. Jones, A. Blanazs and S. P. Armes, *Adv. Mater.*, 2012, **24**, 3378.
23 E. R. Jones, M. Semsarilar, A. Blanazs and S. P. Armes, *Macromolecules*, 2012, **45**, 5091.
24 M. Semsarilar, V. Ladmiral, A. Blanazs and S. P. Armes, *Polym. Chem*., 2014, **5**, 3466.
25 M. Semsarilar, E. R. Jones and S. P. Armes, *Polym. Chem*., 2014, **5**, 195.
26 D. Zehm, L. P. D. Ratcliffe and S. P. Armes, *Macromolecules*, 2013, **46**, 128.
27 W.-M. Wan, C.-Y. Hong and C.-Y. Pan, *Chem. Commun*., 2009, **39**, 5883.
28 W.-M. Wan and C.-Y. Pan, *Polym. Chem*., 2010, **1**, 1475.
29 C.-Q. Huang and C.-Y. Pan, *Polymer*, 2010, **51**, 5115.
30 W.-D. He, X.-L. Sun, W.-M. Wan and C.-Y. Pan, *Macromolecules*, 2011, **44**, 3358.
31 W.-M. Cai, W.-M. Wan, C.-Y. Hong, C.-Q. Huang and C.-Y. Pan, *Soft Matter*, 2010, **6**, 5554.
32 L. A. Fielding, M. J. Derry, V. Ladmiral, J. Rosselgong, A. M. Rodrigues, L. P. D. Ratcliffe, S. Sugihara and S. P. Armes, *Chem. Sci.*, 2013, **4**, 2081.
33 L. Houillot, C Bui, M. Save, B. Charleux, C. Farcet, C. Moire, J.-A. Raust and I. Rodriguez, *Macromolecules*, 2007, **40**, 6500.
34 A. Blanazs, A. J.Ryan and S. P. Armes, *Macromolecules*, 2012, **45**, 5099.
35 P. Chambon, A. Blanazs, G. Battaglia and S. P. Armes, *Macromolecules*, 2012, **45**, 5081.
36 H. Qiu, V. A. Du, M. A. Winnik and I. Manners, *J. Am. Chem. Soc*., 2013, **135**, 17739.
37 N. McGrath, F. H. Schacher, H. Qiu, S. Mann, M. A. Winnik and I. Manners, *Polym. Chem*., 2014, **5**, 1923.
38 M.-S. Hsiao, S. Fairus, M. Yusoff, M. A. Winnik and I. Manners, *Macromolecules*, 2014, **47**, 2361.
39 J. R. Finnegan, D. J. Lunn, O. E. C. Gould, Z. M. Hudson, G. R.; Whittell, M. A. Winnik and I. Manners, *J. Am. Chem. Soc*., 2014, **136**, 13835.
40 X. Zhang, S. Boisse, C. Bui, P. A. Albouy, M.-H. Li, J. Rieger and B. Charleux, *Soft Matter*, 2012, **8**, 1130.
41 A. Blanazs, S. P. Armes and A. J. Ryan, *Macromol. Rapid Commun*., 2009, **30**, 267.
42 S. A. Greenberg and T. Alfrey, *J. Am. Chem. Soc*., 1954, **76**, 6280.
43 F. Fleischhaker, A. P. Haehnel, A. M. Misske, M. Blanchot, S. Haremza and C. Barner-Kowollik, *Macromol. Chem. Phys*., 2014, **215**, 1192.
44 W.-J. Zhang, C.-Y. Hong and C.-Y. Pan, *J. Mater. Chem. A*, 2014, **2**, 7819.
45 A. B. D. Nandiyanto, Y. Akane, T. Ogi and K. Okuyama, *Langmuir*, 2012, **28**, 8616.